International Journal of Research in Medical Sciences
Soorya PS et al. Int J Res Med Sci. 2023 Oct;11(10):3722-3728
www.msjonline.org
pISSN 2320-6071 | eISSN 2320-6012
DOI: https://dx.doi.org/10.18203/2320-6012.ijrms20233026

Original Research Article

Role of magnetic resonance spectroscopy and diffusion-weighted imaging in characterizing intra axial brain tumours

Soorya Prakash S.*, Sudhakar Kattoju

Department of Radiology and Imaging Sciences, Apollo Main Hospital, Chennai, Tamil Nadu, India

Received: 31 July 2023
Revised: 02 September 2023
Accepted: 07 September 2023

***Correspondence:**
Dr. Soorya Prakash S.,
E-mail: sooryaprakash11@gmail.com

ABSTRACT

Background: Magnetic Resonance imaging (MRI) is essential for assessing intracranial malignancies, but conventional MRI has limitations in tumour grading and infiltration information. Advanced Magnetic Resonance (MR) sequences, such as diffusion-weighted (DW) and Magnetic Resonance spectroscopy (MRS), can differentiate between low-grade and high-grade tumours, aiding treatment decisions. This study aims to evaluate the efficacy of diffusion-weighted imaging and magnetic resonance spectroscopy in grading intra-axial brain tumours and correlating the results with histopathology.
Methods: This retrospective study involved 45 patients over one year at Apollo Hospital. MR imaging included conventional sequences, DW, and MRS with localizers in all three planes. DWI and ADC maps were obtained using specific b-values. Standard mean Apparent Diffusion Coefficient (ADC) values were automatically calculated for intra-lesional and peri-lesional regions.
Results: Intralesional ADC values did not significantly differ between high-grade primary tumours (0.4-1 x 10-3 mm^2/s, mean 0.7) and metastases (0.4-0.8 x 10-3 mm^2/s, mean 0.7). However, peri-lesional ADC values were lower in primary tumours (0.3-1.3 x 10-3 mm^2/s, mean 0.8), indicating peri-lesional infiltration, while higher in metastases (1.2-1.6 x 10-3 mm^2/s, mean 1.4) due to the absence of peri-lesional infiltration. Additionally, intralesional ADC values showed a significant difference between low-grade tumours (1-2 x 10-3 mm^2/s) and high-grade tumours (0.4-1 x 10-3 mm^2/s), allowing for their distinction. There were significantly increased Cho/NAA and Cho/Cr ratios in high-grade tumours compared to low-grade tumours.
Conclusions: MR spectroscopy and DWI with computation of ADC values can enhance the diagnostic effectiveness of MR imaging in detecting and grading malignant brain tumours.

Keywords: Apparent diffusion coefficient, Diffusion-weighted images, Intra-axial brain tumour, Magnetic resonance spectroscopy

INTRODUCTION

Magnetic Resonance imaging (MRI) plays a crucial role in evaluating intraaxial brain tumours. It is the most crucial non-invasive technique for cerebral tumour identification, pre-surgical planning, and treatment response evaluation. Although conventional MRI provides a variety of imaging sequences and great soft tissue characterization, it cannot provide information on the grading and infiltration of malignancies.[1]

It is frequently challenging to distinguish between low-grade and high-grade gliomas and neoplastic from non-neoplastic brain masses using conventional MRI, and many instances necessitate biopsy or follow-up imaging.[2,3] In addition to conventional sequences, advanced MR sequences such as MR spectroscopy

(MRS) can increase the effectiveness of MR imaging in diagnosing such tumours.[2] Magnetic resonance spectroscopy can study metabolites and metabolic activity in the brain or neoplasms, giving information on the lesion nature, brain tumour grading and follow-up with treatment responsiveness in these lesions.[4] This technique is a multi-parametrical molecular imaging method that can enable the identification of biochemical patterns of different brain tumours.[5] Diffusion-weighted imaging (DWI) allows us to study more about the brain by observing the minute movements of water molecules. DWI has been utilized to identify the cellularity of brain tumours and distinguish between high- and low-cellular brain tumours.[6] With advanced MR imaging, we can anticipate the chemical makeup of substances, hemodynamic properties, microvascular integrity, and water molecule movement restriction within the mass lesions using MR spectroscopy and diffusion imaging.[7]

MR imaging techniques, such as MR spectroscopy and DWI, can increase the accuracy of diagnosing these tumours. MR Sequences, such as DW and MRS, can distinguish between low-grade and high-grade cancers, aiding the clinician in treatment planning and prognosis assessment.[8] Most studies discuss using an integrated strategy that includes DW imaging, MRS, and conventional sequencing in grading and defining the size of intra-axial brain tumours and their correlation with clinical follow-up and histopathology.

The study's main objectives were to explore the potential of diffusion-weighted imaging (DWI) and MR Spectroscopy (MRS) in differentiating between low-grade and high-grade brain tumours, examine the conventional MRI features associated with cerebral tumours, and establish correlations between imaging observations and final histopathology diagnoses. By achieving these aims, the research aimed to contribute valuable insights into brain tumour grading and diagnostic accuracy.

METHODS

This retrospective study, conducted at Apollo Hospitals Chennai over one year from January to December 2022, focused on clinically diagnosed or suspected patients with intra-axial brain tumours. After applying specific inclusion criteria, 45 patients were selected for analysis. Excluded from the study were cases without intracranial mass on MRI and those with claustrophobia, metallic implants, cardiac pacemakers, and metallic foreign bodies. Additionally, patients with brain tumours caused by infections were not included in the data interpretation.

Data collection

Patients were subjected to a multiplanar, multisequential MRI scan of the brain on an INGENIA 3T MR Machine by Philips in the department of radiodiagnosis and Imaging. The institutional ethical committee accorded ethical clearance to this study. The confirmation of the diagnosis was done histopathologically.

After proper positioning of patients, localisers were taken in coronal, sagittal, and axial planes. The MRI protocol consisted of the following sequences:

In the axial plane: Turbo spin echo (TSE) T2W sequence [repetition time (TR)/echo time (TE)/number of excitations (n) = 3607 ms/100 ms/3], Turbo field echo (TFE) T1W sequence (TR/TE/n = 483 ms/15 ms/1), FLAIR-Fluid attenuated inversion recovery sequence (TR/TE/n = 6000 ms/120 ms/2; inversion time, 2000 ms), SWI sequence (TR/TE= = 23 ms/20 ms), FLAIR sequence in coronal plane and T2W sequence in sagittal plane, contrast-enhanced T1W sequence, diffusion-weighted (DW) imaging using echo planar imaging (EPI) sequence with TR/TE = 3034 ms/100 ms, field of view = 23 cm x 23cm, number of excitations = 3, slice thickness = 5 mm, inter-slice gap = 1.5mm, matrix size = 256 x 256. Diffusion-sensitizing gradients were applied along the three orthogonal directions with diffusion sensitivity values of b = 0 and b = 1000 s/mm^2. Multi-voxel MR spectroscopy was performed using a spin echo mode sequence (SE) with long TE (144 mm/s) and short TE (35 mm/s). Water suppression was achieved with the point-resolved spectroscopy (PRESS) technique. The voxels were placed on the lesions away from CSF and scalp fat to avoid contamination, and the voxel was placed in the normal region. The metabolites were identified, including the following: N-acetyl aspartate (NAA) at 2.0 ppm, creatine (Cr) at 3.0 ppm, choline (Cho) at 3.2 ppm, lipid at the range of 0.7-1.3 ppm, lactate at 1.33 ppm, and myoinositol at 3.56 ppm. The ratios were calculated, including Cho/NAA and Cho/Cr in intralesional regions. The size and position of the voxel were carefully selected to place it well within the lesion, and the spectra were not affected by surrounding healthy tissue.

Statistical analysis

The data was recorded in a proforma and analyzed using descriptive statistics. Various numerical tools like the mean, standard deviation, and p-value were used to analyze the data.

RESULTS

Thirty-three cases were histopathologically diagnosed as gliomas. For analysing the imaging characteristics, glioblastoma Grade IV, oligodendroglioma Grade III, astrocytoma Grade III, and astrocytoma Grade IV were taken as high-grade, and astrocytoma Grade II, oligodendroglioma Grade II, pilocytic astrocytoma, medullary glioma were considered high-grade (Table 1). Nine cases were histopathologically diagnosed as metastasis. Three were histopathologically diagnosed as lymphoma.

On analysis, it was observed that the peak incidence for metastases was in the higher age group (41-50 years), as the case for high-grade glioma with the peak incidence in the age group 51-60 years (Table 2).

Table 1: Distribution of patients according to histopathological diagnosis (n=45).

Type of lesion		No. of lesions	Percentage
Metastases		9	20
High grade glioma	Glioblastoma grade IV	13	28.9
	Oligodendroglioma grade III	2	4.4
	Astrocytoma grade III	1	2.2
	Astrocytoma grade IV	2	4.4
Low grade glioma	Oligodendroglioma grade II	5	11.1
	Astrocytoma grade II	7	15.6
	Pilocytic astrocytoma	2	4.4
	Medullary glioma	1	2.2
Lymphoma		3	6.7

Table 2: Age wise distribution of the lesion (n=45).

	Age groups (years)							
	0-10	**11-20**	**21-30**	**31-40**	**41-50**	**51-60**	**61-70**	**>70**
High grade glioma	-	-	1	2	3	6	5	1
Low grade glioma	1	2	3	4	2	1	2	-
Metastasis	-	-	1	1	3	2	2	-
Lymphoma	-	-	-	2	1	-	-	-

Table 3: Imaging characteristics of intra axial brain tumours.

Parameters	Tumour grade, N (%)				P value#
	Glioma		Metastasis	Lymphoma	
	High grade	Low grade			
T1					
Hypointense	14 (77.8)	12 (80)	5 (55.6)	3 (100)	0.783
ISO intense	3 (16.7)	2 (13.3)	3 (33.3)	-	
Heterointense	1 (5.6)	1 (6.7)	1 (11.1)	-	
T2					
Hyperintense	6 (33.3)	13 (86.7)	7 (77.8)	2 (66.7)	0.011
Heterointense	12(66.7)	2 (13.3)	1 (11.1)	-	
Hypointense	-	-	-	1 (33.3)	
ISO intense	-	-	1 (11.1)	-	
Flair					
Hyperintense	6 (33.3)	13 (86.7)	7 (77.8)	2 (66.7)	0.011
Heterointense	12(66.7)	2 (13.3)	1 (11.1)	-	
Hypointense	-	-	-	1 (33.3)	
ISO intense	-	-	1 (11.1)	-	
Diffusion Restriction					
Present	17 (94.4)	3 (20)	9 (100)	3 (100)	<0.001
Absent	1 (5.6)	12 (80)	-	-	
Blooming SWI					
Present	13 (72.2)	1 (6.7)	-	-	<0.001
Absent	5 (27.8)	14 (93.3)	9 (100)	3 (100)	
Contrast enhancement					
Peripheral	10 (55.6)	5 (33.3)	6 (66.7)	1 (33.3)	0.143
Hetero	6 (33.3)	4 (26.7)	3 (33.3)	2 (66.7)	
Absent	2 (11.1)	6 (40)	-	-	

Out of 15 cases of low-grade gliomas, 13 (86.7%) were hyperintense on T2WI, and 14 (93.3%) were ISO/ hypointense on T1WI. Blooming on SWI imaging was seen in 1 case (6.7%). On contrast enhancement, heterogenous enhancement in 5 (33.3%), peripheral enhancement was seen in 4 (26.7%) and was absent in 6 (40%). Out of 18 cases of high-grade glioma, 17 (94.5%) were isointense/hypointense on T1WI, and 12 (66.6%) were heterogenous on T2WI. Blooming on SWI was noted in 13 (72.2%), diffusion restriction in 17 (94.4%), heterogenous enhancement in 6 (33.3%), peripheral enhancement in 10 (55.6%) and absent in 2 (11.1%). Out of 9 cases of metastases, 8 (88.8%) were isointense/hypointense on T1WI, and 7 (77.7%) were hyperintense on T2WI. Blooming on SWI was noted in 4 (44.4%), diffusion restriction in 9 (100%), heterogenous enhancement in 3 (33.3%) and peripheral enhancement in 6 (66.6%) cases. All cases of lymphoma showed diffusion restriction and no blooming on SWI. Lactate peak was seen in 7 (77.8%) cases of metastasis, 10 (55.5%) cases of high-grade glioma and 2 (13.3%) cases of low-grade glioma (Table 3).

Table 4: Comparison of MR Spectroscopy findings with final histopathological diagnosis.

Histopathology	MRI spectroscopy, Mean±SD (range)								
	N-Acetyl Aspartate			Choline			Creatinine		
	Lesion	Control	P value*	Lesion	Control	P value*	Lesion	Control	P value*
High grade glioma	3.1±1.6 (1.3-8)	11.1±3.2 (7.5-17)	<0.001	12±3.2 (6.2-17.4)	3.4±0.7 (2.3-4.8)	<0.001	4±1.8 (1.9-8)	3.4±0.5 (2.2-4.6)	0.096
Low grade glioma	5.4±1.8 (3.1-8.4)	10.9±2.1 (7.3-14)	<0.001	8.8±2.6 (4.2-14.3)	3.9±0.9 (3.2-6)	<0.001	5±1.7 (3.1-8.5)	3.8±0.8 (2.8-5.7)	0.012
Metastasis	2.6±0.4 (2.2-3.4)	10.7±1.9 (7.8-14)	<0.001	9.4±1.4 (7.3-12)	3.2±0.5 (2.5-3.8)	<0.001	2.9±0.3 (2.1-3.3)	3.2±0.6 (2.3-3.8)	0.206
Lymphoma	2.3±0.4 (1.9-2.6)	10.3±1.7 (8.6-12)	0.001	11.6±3.4 (8.5-15.3)	3.1±0.7 (2.4-3.7)	0.014	3±0.8 (2.1-3.6)	3.2±0.5 (2.8-3.8)	0.781

Table 5: Intralesional Cho/NAA and Cho/Cr ratio among studied cases.

Ratio	Tumour Grade				P value#
	Glioma		Metastasis	Lymphoma	
	High Grade	Low Grade			
Cho/NAA, Mean±SD	4.3±1.5	1.7±0.6	3.7±0.9	4.8±0.8	<0.001
Range	1.8-7	1.1-2.7	2.7-5.2	4.4-5.7	
Cho/Cr, Mean±SD	3.4±1.0	1.8±0.5	3.2±0.3	3.8±0.8	<0.001
Range	1.3-5.2	1-2.7	2.6-3.6	2.9-4.5	

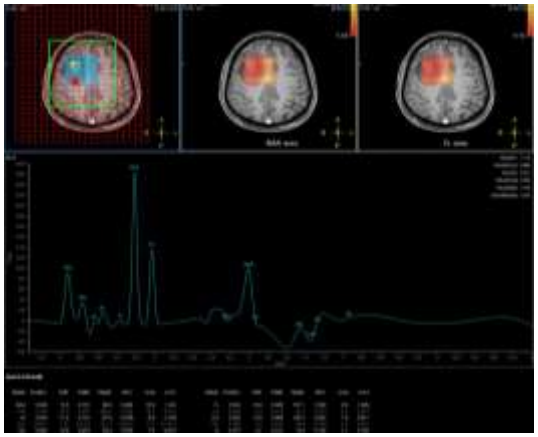

Figure 1: MR spectroscopy graph in a case of Glioblastoma grade IV showing markedly elevated choline peak with very low NAA peak and Cho/NAA ratio is 3.1.

MR spectroscopy was done in all cases. Statistically significant increase in choline and reduction in NAA levels with significantly elevated Cho/NAA and Cho/Cr was found in high-grade glioma compared to low-grade glioma (Table 4, 5) (Figure 1).

In metastases, a significant reduction in the NAA levels was noted. In lymphoma cases, reduced NAA and raised choline were also seen (Table 4).

Apparent diffusion coefficient (ADC) values of tumoural and peritumoural regions were compared. Patients with high-grade glioma and metastases had significantly lower ADC (mean= 0.7x 10-3mm^2/s) in the tumoural region as compared to low-grade gliomas (mean= 1.4 x 10-3mm^2/s) with p-value <0.0001. ADC values of lymphoma (mean= 0.5 x 10-3mm^2/s) were lower than that of high-grade glioma in the tumoural region (Table 6) (Figure 2A, 2B).

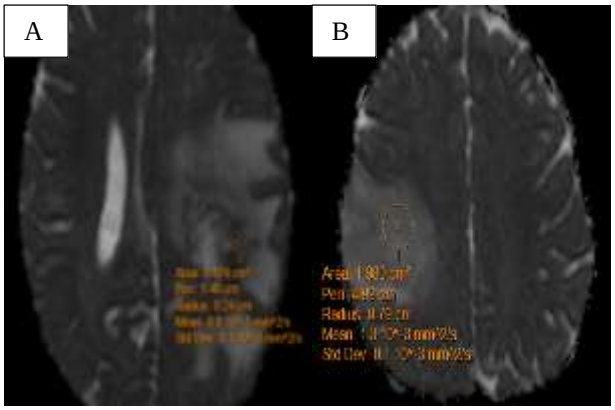

Figure 2: ADC map. 2A) ADC map in a case of glioblastoma grade IV shows reduced ADC value of 0.8 suggesting high grade lesion. 2B) ADC map in a case of oligodendroglioma grade II shows elevated ADC value of 1.3 suggesting low grade lesion.

Perilesional ADC values calculated around tumour areas were higher in metastasis, denoting no perilesional infiltration (1.4x10-3mm^2/s) than high-grade primary tumour (0.8x10-3mm^2/s), denoting perilesional infiltration (Table 6).

Table 6: Comparison of ADC values with final histopathological diagnosis.

MRI diagnosis	DW imaging	
	ADC, Mean±SD (Range)	
	Tumour	Peritumour
High grade glioma	0.7±0.3 (0.4-1)	0.8±0.3 (0.3-1.3)
Low grade glioma	1.4±0.3 (1-2)	1.5±0.2 (1.1-1.9)
Metastasis	0.7±0.1 (0.4-0.8)	1.4±0.1 (1.2-1.6)
Lymphoma	0.5±0.1 (0.5-0.6)	0.6±0.1 (0.5-0.7)

DISCUSSION

For the initial assessment of intra-axial brain tumours, conventional magnetic resonance imaging is still the basic imaging required as it provides fundamental details about these tumours' anatomical characteristics, such as oedema, mass effect, and pattern of enhancement.[10]

The use of invasive diagnostic techniques like brain biopsies is limited by MRS. MRS offers a qualitative study of a number of compounds within the brain, in contrast to the structural data offered by MRI.[11] These compounds show characteristics of the growth or degeneration of cell membranes, energy consumption, and necrotic transformation of brain or tumour tissue.[12] According to our MRS findings, all of them displayed varying degrees of elevated choline peak and CHO/NAA ratios using long TE (144 msec), with considerable increases from both low-grade and high-grade tumours, with no discernible difference between primary high-grade tumours and metastatic brain tumours. This was in accordance with the findings of Martinez-Bisal and Celda and Shokry that increased CHO/NAA ratios in lesions could only distinguish between low-grade and high-grade primary tumours.[13,10] The results of Delorme and Weber were further supported by the decreasing Cr peak found in all cases, with a substantial increase from low-grade to high-grade tumours but without a discernible difference between primary and metastatic brain tumours.[14]

In the short (TE 35 ms), the lactate levels did not significantly differ between primary and metastatic brain tumours, but they did significantly differ between low-grade and high-grade tumours. This conclusion was consistent with Van der Graaf's assertion that lactate peaks typically indicate aggressive tumours, showing enhanced anaerobic metabolism and cellular necrosis and that the pathogenesis of primary and metastatic brain tumours is quite similar.[15] Short (TE 35 ms) demonstrated greater lipid peaks in metastatic brain tumours. This was in agreement with Shokry, Opstad et al, and Van der Graaf, who suggested that cancer cells of various origins contain mobile, spectroscopically detectable lipids in their cell membranes, which could account for the higher lipid levels in metastatic lesions.[10,16,15] Another significant finding from this study was that intralesional voxels in primary tumours displayed various degrees of CHO/Cr ratios, which increased as the tumour's grade increased.

As a result, CHO/Cr ratios have consistently predicted tumour grade. A substantial difference between high- and low-grade tumours was found when comparing CHO/Cr ratios between the two groups. The difference between the CHO/Cr ratios reported in high-grade and low-grade tumours was substantially connected with the expression of proliferating cells, according to Chen et al and Faria et al.[17,18]

In this study, there is no significant difference in intralesional ADC values between metastatic and primary brain tumours, and we cannot differentiate metastatic brain tumours from primary brain tumours by intralesional ADC values only. This result matched with Pavlisa et al, Lee et al and Ohba et al, which referred to this result due to the increase in the cellularity of all these lesions to the level that DWI could not differentiate.[19-21]

Another important finding was that intralesional ADC values were significantly different for low-grade and high-grade tumours, ranging from 1 to 2 x 10-3 mm^2/s for low-grade tumours and 0.4 to 1 x 10-3 mm^2/s for high-grade tumours. Therefore, we could distinguish between low-grade and high-grade tumours in our investigation using ADC values. This finding was consistent with Ohba et al, who also noted that ADC values could be used to grade primary tumours.[21]

In this study, perilesional ADC values were elevated in metastatic brain tumours than in primary high-grade tumours, with significant ADC value changes between these tumours. Perilesional ADC values calculated around the lesion were higher in metastasis (vasogenic oedema), denoting no perilesional infiltration (1.2-1.6 x 10-3 mm^2/s) than high-grade primary tumours (0.3-1.3 x 10-3 mm^2/s) denoting peri lesion infiltration. So in the current study, we can differentiate primary from metastatic brain tumours based on peritumoral ADC values. This was consistent with the findings of Faria et al, who attributed these findings to the perilesional infiltration of primary high-grade tumours, which increases cellularity in the perilesional area, as opposed to metastatic tumours, which exhibit no perilesional infiltration and shows increased ADC values in perilesional oedema.[18] In our study, high-grade malignant tumours exhibited the lowest ADC values based on primary tumoural area calculations. The ADCs of the various tumour types in the same grade did not differ in any way, according to our study. Clinical significance: Conventional MRI sequences are limited in their ability to grade tumours and define tumour infiltration, which makes surgical removal and post-operative care more difficult. The present study suggests that characterising tumours and surrounding tissue using sophisticated MRI techniques like DW Imaging and spectroscopy is possible based on water diffusion and the presence of metabolites. This information aids clinicians in better-managing malignancies and also helps with differential diagnosis in ambiguous tumours.

Our study's main limitation was its small sample size, particularly when the information was evaluated independently for various tumour types. More research is required to identify the cutoff values of ADC, metabolite concentrations, and ratios in specific cancers.

CONCLUSION

According to the results of our study, MR spectroscopy and DWI with computation of ADC values could increase the diagnostic effectiveness of MR imaging in detecting and grading malignant brain tumours. Intralesional ADC measurements are not useful for distinguishing between primary and metastatic tumours. ADC levels at the perilesional region can distinguish between primary and metastatic brain tumours. Lesions that exhibit similar characteristics on conventional MRI may be distinguished using MRS. The most precise marker for intracranial tumours is choline. Increases in choline levels and choline/NAA ratios strongly signal that the neoplasm is malignant and should be graded and monitored to determine tumour response to treatment.

ACKNOWLEDGEMENTS

Authors would like to thank Mr. Logesh, Bio-statistician, and Dr. Shivashankari, Research assistant for their constant support and guidance.

Funding: No funding sources
Conflict of interest: None declared
Ethical approval: The study was approved by the Institutional Ethics Committee of Bio Medical Research-Apollo Hospitals, Chennai, Tamil Nadu

REFERENCES

1. Svolos P, Kousi E, Kapsalaki E, Theodorou K, Fezoulidis I, Kappas C, et al. The role of diffusion and perfusion weighted imaging in the differential diagnosis of cerebral tumours: a review and future perspectives. Cancer Imag. 2014;14(1):20.
2. Bulakbasi N, Kocaoglu M, Ors F, Tayfun C, Uçöz T. Combination of single-voxel proton MR spectroscopy and apparent diffusion coefficient calculation in the evaluation of common brain tumours. AJNR Am J Neuroradiol. 2003;24(2):225-33.
3. Chiang IC, Kuo YT, Lu CY, Yeung KW, Lin WC, Sheu FO, et al. Distinction between high-grade gliomas and solitary metastases using peritumoural 3-T magnetic resonance spectroscopy, diffusion, and perfusion imagings. Neuroradiol. 2004;46(8):619-27.
4. Smith JK, Castillo M, Kwock L. MR spectroscopy of brain tumours. Mag Resonan Imag Clin North Ame. 2003;11(3):415-29.
5. Dawoud MAE, Sherif MF, Eltomey MA. Apparent diffusion coefficient and Magnetic resonance spectroscopy in grading of malignant brain neoplasms. Egypt J Radio Nucl Medi. 2014;45(4):1215-22.
6. Yamasaki F, Kurisu K, Satoh K, Arita K, Sugiyama K, Ohtaki M, et al. Apparent diffusion coefficient of human brain tumours at MR imaging. Radiol. 2005;235(3):985-91.
7. Naser RKA, Hassan AAK, Shabana AM, Omar NN. Role of magnetic resonance spectroscopy in grading of primary brain tumours. Egypt J Radiol Nucl Medi. 2016;47(2):577-84.
8. Gupta K, Jain N, Saggar K. Role of diffusion weighted imaging and MR spectroscopy in characterisation of intracranial neoplasms. Int J Anat Radiol Surg. 2018;7(3):RO55-61.
9. Louis DN, Perry A, Wesseling P, Brat DJ, Cree IA, Figarella-Branger D, et al. The 2021 WHO classification of tumours of the central nervous system: a summary. Neuro-Oncol. 2021;23(8):1231-51.
10. Shokry A. MRS of brain tumours: Diagrammatic representations and diagnostic approach. Egypt J Radio Nucl Medi. 2012;43(4):603-12.
11. Darwiesh AMN, Maboud NMAE, Khalil AMR, ElSharkawy AM. Role of magnetic resonance spectroscopy and diffusion weighted imaging in differentiation of supratentorial brain tumours. Egypt J Radiol Nucl Medi. 2016;47(3):1037-42.
12. Sibtain NA, Howe FA, Saunders DE. The clinical value of proton magnetic resonance spectroscopy in

adult brain tumours. Clin Radiol. 2007;62(2):109-19.
13. Martínez-Bisbal MC, Celda B. Proton magnetic resonance spectroscopy imaging in the study of human brain cancer. Q J Nucl Med Mol Imag. 2009;53(6):618-30.
14. Delorme S, Weber M. Applications of MRS in the evaluation of focal malignant brain lesions. Cancer Imag. 2006;6(1):95-9.
15. Van Der Graaf M. In vivo magnetic resonance spectroscopy: basic methodology and clinical applications. Eur Biophys J. 2010;39(4):527-40.
16. Opstad KS, Murphy MM, Wilkins PR, Bell BA, Griffiths JR, Howe FA. Differentiation of metastases from high-grade gliomas using short echo time1H spectroscopy. J Magn Reson Imag. 2004;20(2):187-92.
17. Chen J, Huang SL, Li T, Chen XL. In vivo research in astrocytoma cell proliferation with 1H-magnetic resonance spectroscopy: correlation with histopathology and immunohistochemistry. Neuroradiol. 2006;48(5):312-8.
18. Faria AV, Macedo FC, Marsaioli AJ, Ferreira MMC, Cendes F. Classification of brain tumour extracts by high resolution 1H MRS using partial least squares discriminant analysis. Braz J Med Biol Res. 2011;44(2):149-64.
19. Pavlisa G, Rados M, Pavlisa G, Pavic L, Potocki K, Mayer D. The differences of water diffusion between brain tissue infiltrated by tumour and peritumoural vasogenic edema. Clin Imag. 2009;33(2):96-101.
20. Lee EJ, TerBrugge K, Mikulis D, Choi DS, Bae JM, Lee SK, et al. Diagnostic value of peritumoural minimum apparent diffusion coefficient for differentiation of glioblastoma multiforme from solitary metastatic lesions. AJR Am J Roentgenol. 2011;196(1):71-6.
21. Ohba S, Nakagawa T, Murakami H, Ushioda T, Shimizu K. Diffusion magnetic resonance imaging for enhanced visualization of malignant cerebral tumours and abscesses. Neurol India. 2011;59(5):674.

Cite this article as: Soorya PS, Kattoju S. Role of magnetic resonance spectroscopy and diffusion-weighted imaging in characterizing intra axial brain tumours. Int J Res Med Sci 2023;11:3722-8.